Simulation of Convective Heat Transfer in 3D Forward Facing Step Using Various Turbulence Models

Raj Sarath & Janardanan Sarasamma Jayakumar*

Department of Mechanical Engineering, Amrita Vishwa Vidyapeetham,
Amritapuri, Kollam 690525, India
*E-mail: jsjayan@gmail.com

Highlights:

- Numerical simulations were performed using a newly developed transient solver, pisoTempFoam.
- For the *k-ε* and v^2*-f* turbulence models, the recirculation length in the upstream region increased by 6.97% with an increase in step height.
- Increasing Re from 5,000 to 10,000, the recirculation length in the upstream region increased by 48.6% and 49.2% for the *k-ω* and *k-ω SST* models, respectively.
- As the Prandtl number was increased, the *k-ω* and *k-ω SST* models over-predicted the recirculation length in the downstream region.

Abstract. In this work, a modified solver from the OpenFOAM 4.1 software was used to study the fluid flow and heat transfer characteristics over a forward facing step (FFS) considering various turbulence models, viz., *k-ε*, *k-ω*, *k-ω SST* and v^2*-f*. Numerical computations were performed using a newly developed transient solver, pisoTempFoam. Modeling and meshing of the geometry and setting of the boundary conditions were done with OpenFOAM. The bottom (upstream, step and downstream) walls were heated at a constant temperature of 350K, while the fluid inlet temperature was 298K. The simulation results were compared with those available in the literature. Variation of skin friction coefficient (C_f), coefficient of pressure (C_p), and Nusselt number (Nu) for different Reynolds numbers (Re), contraction ratios (CR) and different fluids are presented. This article also presents information about recirculation bubbles in the upstream and downstream regions of the FFS. The results show that the combined effect of turbulence models and parameters, such as CR, Re and Pr, change the flow and heat transfer characteristics of the FFS. The present CFD simulation plays a pivotal role in the analysis of flow over airfoils at a large angle of attack in heat exchangers and pipes whose area suddenly changes.

Keywords*: forward facing step; heat transfer; k-epsilon; k-omega; k-omega SST; v^2-f; turbulence model; pisoTempFoam; OpenFOAM.*

1 Introduction

Flow over sudden contractions and expansions are found in day-to-day life and in many engineering applications. The cooling of electronic modules, the

Received September 16th, 2019, 1st Revision February 26th, 2020, 2nd Revision July1st, 2020 Accepted for publication August 4th, 2020.

DOI: 10.5614/j.eng.technol.sci.2020.52.5.2

functioning of compact heat exchangers, various heat transfer enhancements, etc. fall under this category. In addition, this phenomenon can also be found in various flow separation and reattachment zones of high-performance boilers, heat exchangers and cooling passages of turbine blades. Such phenomena can be accurately modeled and analyzed by considering them as backward or forward-facing steps. Studies have revealed that an antagonistic and unfavorable pressure gradient exists in the flow over backward facing steps (BFS) and forward-facing steps (FFS). Due to this pressure gradient, the flow gets separated and reattached in sudden expansion and contraction regions near to the step [1]. Heat transfer variations due to the above-mentioned flow separations and reattachments may cause failure in equipment in certain cases. Studies have shown that in FFS, depending on the ratio of boundary layer thickness to step height, recirculation bubbles can form in the upstream and downstream regions [1]. Therefore, the flow becomes more complicated in FFS compared to BFS. Hence, the usage of a proper turbulence model is necessary for defining the flow and heat transfer characteristics in FFS.

In the past, several techniques have been developed to simulate complex flow and heat transfer problems in both BFSs and FFSs. Jayakumar, *et al*. [2] carried out numerical analysis on an FFS using the hybrid mesh finite volume CFD code. They used two turbulence models, k-ε and k-ω, and investigated the conjugate heat transfer within an FFS. Sajesh & Jayakumar [3] investigated the flow and heat transfer characteristics over a 3D BFS. They analyzed the effects of streamline curvature on C_f, C_p and Nu using k-ω *SST* turbulence model at a Re value of 80000. Vijay, *et al.* [4] numerically investigated the flow over a double forward facing step using the ANSYS-17 software package. From the analysis, the authors concluded that when the Reynolds number and distance between the steps were increased, the 3D effects became more predominant. Togun, *et al*. [5] carried out a numerical analysis with the commercial CFD package ANSYS 14 ICEM. Using the k-ε turbulence model and a Re value ranging from 30,000 to 100,000, they analyzed variations in Nu and pointed out that the heat transfer rate increased with increasing step height. Considering a water-functionalized multi-walled carbon nanotube as the working fluid, Safaei, *et al*. [6] and Alrashed, *et al*. [7] carried out numerical analyses for studying the convective heat transfer in overheated FFSs and BFSs. For analyzing different flow and heat transfer characteristics over a microscale forward facing step, Kherbeet, *et al.* [8] conducted numerical studies. In order to study the flow through a compound channel Nugroho & Ikeda [9] carried out experimental and numerical analyses. The numerical analysis was carried out with the Large Eddy Simulation Sub Depth Scale model. The authors analyzed the variations of the longitudinal wavelength of vortices created within the flow field. Using the k-ε turbulence model Kusuma, *et al*. [10] conducted a numerical analysis for finding the recirculation patterns within a scaled-down 2D reservoir. By experimental

analysis Li, *et al*. [11] found out the effect of various frequencies of disturbances within the flow field on the heat transfer rate in the flow attachment and recirculation regions of a BFS. Hilo, *et al*. [12] numerically investigated variations in the flow and heat transfer characteristics over a corrugated heated downstream wall of a BFS. The authors concluded that the combined effect of wall corrugation and the backward facing step enhanced the heat transfer rate up to 62%.

We know that the usage of a proper turbulence model is very important for the prediction of the fluid flow and heat transfer characteristics in FFSs. To the best knowledge of the authors no published work dealing with a comparison of heat transfer characteristics considering different turbulence models of a three-dimensional FFS is available. In the present work, fluid flow and heat transfer in a 3D FFS were analyzed by using various turbulence models, viz., *k-ε*, *k-ω*, *k-ω SST* and v^2*-f*. The current work presents information about the recirculation regions in the upstream and downstream parts of the forward facing step. Variations of skin friction coefficient (C_f), coefficient of pressure (C_p) and Nusselt number (Nu) are reported for different Reynolds numbers, contraction ratios and fluids. The current work helps to compare and understand the fluid flow and heat transfer characteristics of FFSs for various turbulence models. The open source CFD code OpenFOAM 4.1 was used for this analysis. The usage of commercial CFD code for analyzing the present problem may not be a good choice because they are very expensive and incorporation of suitable models is difficult. Using the open source software OpenFOAM is a good alternative. The present CFD simulation plays a pivotal role in the analysis of flow over airfoils at a large angle of attack in heat exchangers and pipes whose area suddenly decreases.

2 Governing Equations

For a heated 3D FFS, the continuity, momentum (x, y, and z-momentum) and energy equations are written as follows (Eq. (1) to (5)) See [2-4]:

$$\frac{\partial \rho}{\partial t}+\frac{\partial(\rho u)}{\partial x}+\frac{\partial(\rho v)}{\partial y}+\frac{\partial(\rho w)}{\partial z}=0 \tag{1}$$

$$\frac{\partial(\rho u)}{\partial t}+\frac{\partial(\rho uu)}{\partial x}+\frac{\partial(\rho uv)}{\partial y}+\frac{\partial(\rho uw)}{\partial z}=\frac{\partial \tau_{xx}}{\partial x}+\frac{\partial \tau_{yx}}{\partial y}+\frac{\partial \tau_{zx}}{\partial z}-\frac{\partial P}{\partial x}+\rho g_x \tag{2}$$

$$\frac{\partial(\rho v)}{\partial t}+\frac{\partial(\rho vu)}{\partial x}+\frac{\partial(\rho vv)}{\partial y}+\frac{\partial(\rho vw)}{\partial z}=\frac{\partial \tau_{xy}}{\partial x}+\frac{\partial \tau_{yy}}{\partial y}+\frac{\partial \tau_{zy}}{\partial z}-\frac{\partial P}{\partial y}+\rho g_y \tag{3}$$

$$\frac{\partial(\rho w)}{\partial t}+\frac{\partial(\rho wu)}{\partial x}+\frac{\partial(\rho wv)}{\partial y}+\frac{\partial(\rho ww)}{\partial z}=\frac{\partial \tau_{xz}}{\partial x}+\frac{\partial \tau_{yz}}{\partial y}+\frac{\partial \tau_{zz}}{\partial z}-\frac{\partial P}{\partial z}+\rho g_z \tag{4}$$

Here, τ_{xx}, τ_{yy} and τ_{zz} are the normal stresses, which can be written as follows: $\tau_{xx}=-\overline{\rho u'^2}$ $\tau_{yy}=-\overline{\rho v'^2}$ $\tau_{zz}=-\overline{\rho w'^2}$. $\tau_{xy}=\tau_{yx}=-\overline{\rho u'v'}$ $\tau_{xz}=\tau_{zx}=-\overline{\rho u'w'}$ are the three shear stresses.

$$\frac{\partial(\rho C_p T)}{\partial t}+\frac{\partial(\rho C_p uT)}{\partial x}+\frac{\partial(\rho C_p vT)}{\partial y}+\frac{\partial(\rho C_p wT)}{\partial z}=\frac{\partial}{\partial x}\left(k_{eff}\frac{\partial T}{\partial x}\right)+\frac{\partial}{\partial y}\left(k_{eff}\frac{\partial T}{\partial y}\right)+\frac{\partial}{\partial z}\left(k_{eff}\frac{\partial T}{\partial z}\right)+S_T \tag{5}$$

In Eq. (5) k_{eff} is the thermal conductivity (diffusion coefficient), which can be written as $k_{eff}=k+k_t$, where k and k_t are the thermal conductivity and the turbulent thermal conductivity of the fluid respectively. Here, k_t is calculated by $k_t=\frac{\mu_t C_p}{\mathrm{Pr}_t}$, where Pr_t is the turbulent Prandtl number, the value of which ranges from 0.7 to 0.9. Since no heat generation is considered within the domain, the source term S_T is not considered in the new solver. The existing solver code pisoFoam of OpenFOAM 4.1 was modified by adding Eq. (5) to create the new transient incompressible solver, pisoTempFoam. The finite volume method (FVM) [2] was used for the discretization of the continuity, momentum and energy equations. The transport equations for turbulence kinetic energy and the dissipation rate of turbulence models *k-ε*, *k-ω*, *k-ω SST* and v^2-*f* are available in References [2] and [3].

3 Validation

For validating the methodology of the newly developed solver pisoTempFoam, the experimental work of Vogel and Eaton [1] was considered. In their analysis, Vogel and Eaton [1] focused only on the heated downstream wall of a BFS with expansion ratio 1.25 and analyzed variations of C_f and the Stanton number on the downstream wall. The reference velocity considered in the experiment was 11.3 m/s, corresponding to a Re value of 28,000. From Figure 1 it is clear that the C_f variations had good agreement in the back-flow region of recirculation and in the reattachment region, i.e. at a distance of 0 to 7 cm.

In the region between 15 and 20 cm (downstream region) the numerical results also showed good agreement with Vogel and Eaton [1]; the relative error was

within 5%. However, the results showed poor agreement in the step region (10 to 15 cm) where the flow area suddenly expands. The resulting adverse pressure gradient plays a major role in delivering the poor results for this region. It has been reported that the uncertainty in experimental measurement of C_f is in the order of 0.1 times the step height [1]. Considering these factors, the numerical results were in good agreement with the experimental results. Turbulence models k-ε and v^2-f showed the same result, whereas k-ω and k-ω SST slightly over-predicted the variation of C_f values.

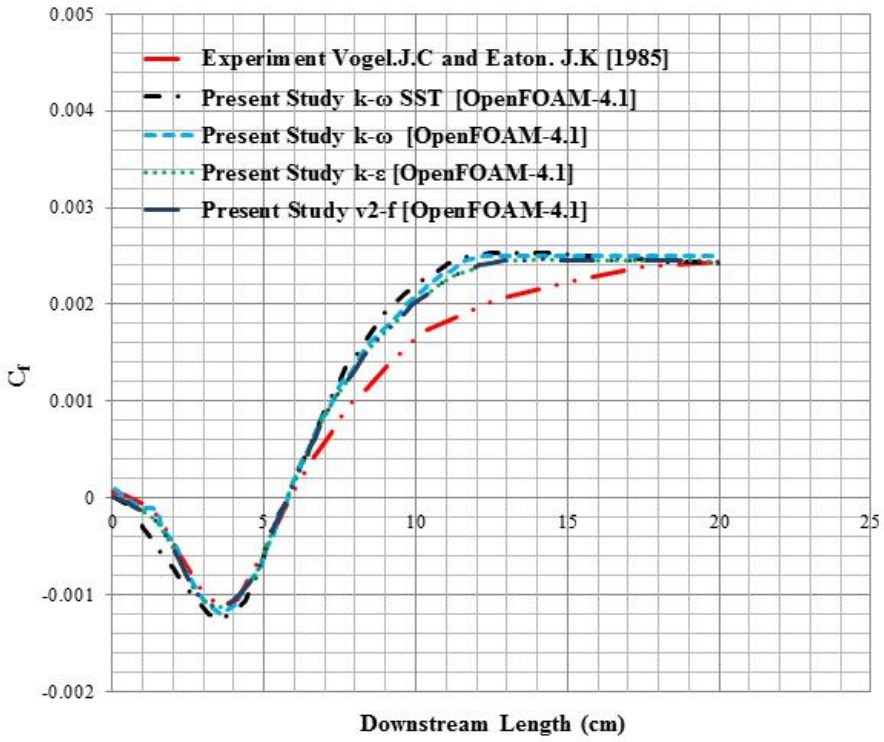

Figure 1 Variation of skin friction coefficient along the heated bottom wall.

4 Geometry Description and Solution Methodology

The numerical study was conducted for turbulent flow and heat transfer over a forward facing step of 3 m length (along the x-axis), 1 m height (along the y-axis), and 1 m width (along the z-axis). The geometry considered for the simulation is shown in Figure 2. The inlet was defined as a velocity inlet and the velocity values were calculated from the Reynolds number (Re). The inlet fluid temperature (Tc) was 298 K. The step height, s, was varied based on the contraction ratio.

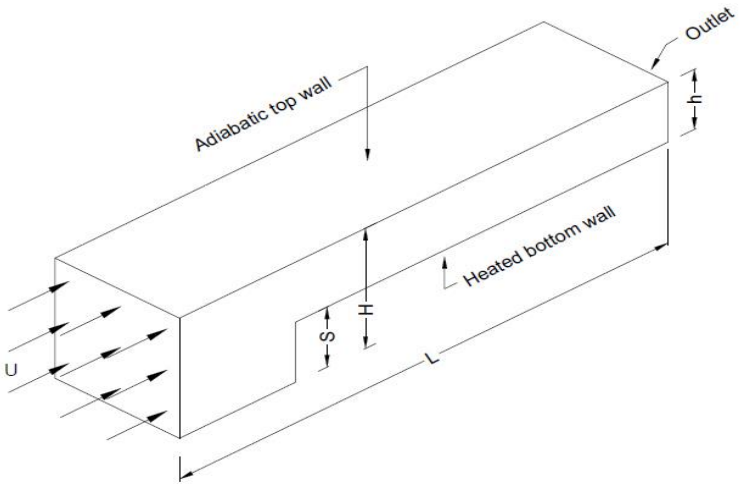

Figure 2 Geometry details of 3D FFS.

Figure 3 shows the flow chart of the solution procedure used in the numerical study. The procedure starts with preparation of the mesh using the blockMesh utility of OpenFOAM [13,14]. The transport and thermodynamic properties of fluids are defined in the files 'thermophysicalProperties' and 'transportProperties' in the case folder. The initial and boundary conditions for fields such as *p, T, U, k,* ε and ω are defined in the time directory of the case file. Solution controlling factors such as time step (δt), end time (E_t) and number of iterations in the PISO algorithm [3] are specified in the files 'controlDict' and 'fvSolution''. The files 'fvSchemes' and 'fvSolution' in the case file include details regarding the discretization schemes and solvers used for solving the different governing equations. For spatial and temporal discretization, the modified solver pisoTempFoam uses the finite volume Gaussian linear integration and implicit Euler methods, respectively. The velocity term and all the turbulence fields are solved with smoothSolver and the preconditioner used is Gauss-Seidel.

The pressure field is solved with the Generalized Geometric Algebraic Multi-grid (GAMG) solver with Gauss-Seidel preconditioner. The pressure and velocity fields are coupled using the Pressure Implicit with Splitting of Operators (PISO) algorithm. The temperature and all turbulence fields are solved with the smoothSolver solver with GaussSeidel preconditioner. The temporal and spatial terms are discretised using the above mentioned schemes in functions '*ddt*( )', '*div*( )' and '*laplacian*( )' from the '*fvm*' class in OpenFOAM. After discretisation, the system of equations for each field is obtained. This is assembled using the '*fvMatrix'* class and solved. This procedure is continued until

the specified end time (E_t). After reaching the specified end time, the results are post-processed using the open source visualization package paraView.

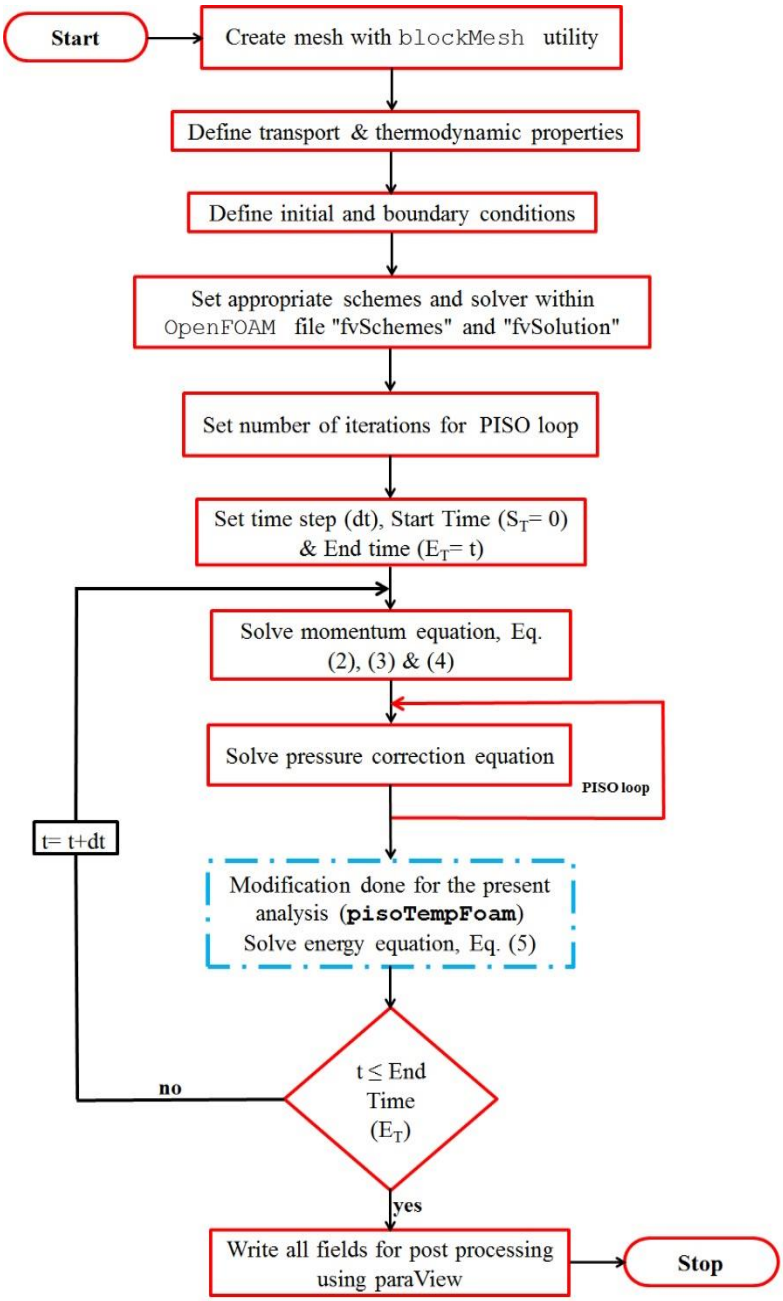

Figure 3 Solution procedures for the present analysis.

5 Results and Discussion

The present work deals with the effect of geometrical parameters, properties of the working fluid and velocity of inlet gas on the flow and heat transfer characteristics of a 3D FFS. In order to study the effect of CR, three step height values were considered, viz., 0.15 m, 0.30 m and 0.45 m. Simulations with various values of CR were carried out for Pr = 0.71 and Re = 7000. For analyzing the effect of inlet gas velocity, three Re values were used, viz., 5000, 7000 and 10,000.

By keeping CR at a constant value (CR = 0.55) corresponding to the Reynolds number, the inlet gas velocity was changed. Air (Pr = 0.71) was considered as the working fluid. In order to study the effect of the Pr values, the authors changed different thermophysical properties and kept CR and Re at constant values of 0.7 and 7000 respectively.

5.1 Contraction Ratio

This section explains the effect of CR on different flow and heat transfer characteristics over the heated 3D FFS. Air was considered as the working fluid. Figure 4(a)-(c) show flow visualizations of the upstream region for different CR values. It is clear that the recirculation length increased with step height and thus the heat transfer rate was enhanced.

From the numerical analysis it can be seen that when using the k-ε and v^2-f turbulence models with an increment of step height, the recirculation length in the upstream region increased by 6.97%. However, for the k-ω and k-ω *SST* models, the increment of the recirculation length with an increase in step height was in the order of 23.96% and 25.63%, respectively.

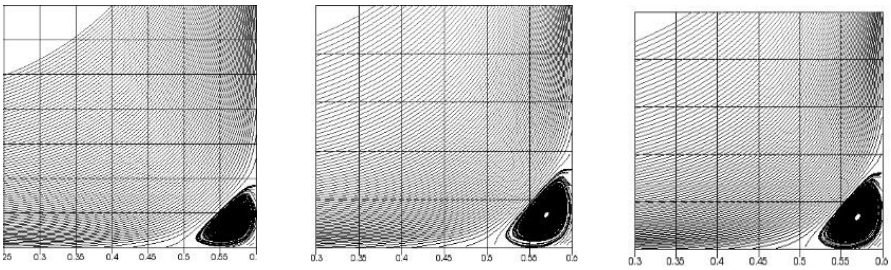

(a) (b) (c)

Figure 4 (a)-(c) Velocity streamline in the upstream region for the k-ε model. (a) CR = 0.85, (b) CR = 0.70, (c) CR = 0.55; (a)-(c) Re = 7000, Pr = 0.71.

The values of the recirculation length in the upstream region for different values of CR are given in Table 1. Figures 5 (a)-(c) show a streamline plot for velocity

in the downstream region. It can be seen that the recirculation zone had the same nature as in the upstream region, i.e. with an increase in step height the recirculation zone became more prominent and its length increased.

The flow visualization of the downstream region shows that for the k-ε and v^2-f turbulence models, the values of the recirculation length were almost the same. However, for the k-ω and k-ω *SST* models the values changed, which could be due to the higher non-linearity of these models. At CR = 0.85, as compared to the other two models, k-ω and k-ω *SST* over-predicted the nature of recirculation in the downstream region. Therefore, for these models (k-ω and k-ω *SST*), the C_f values were higher and the recirculation bubbles were more protuberant.

From the quantitative results it can be seen that in the downstream region when using the k-ε and v^2-f turbulence model with an increment in step height the recirculation length increased by 27.23% and 29.21%, respectively. When increasing the step height and using the k-ω and k-ω *SST* models, the increment of the recirculation length in the downstream region was in the order of 31.61% and 40.56%, respectively.

Table 1 Recirculation lengths considering different CR, Re and Pr values.

			k-ε	k-ω	k-ω *SST*	v^2-f
Contraction Ratio	**CR 0.85**	XRL/s (Upstream)	3.27	1.95	1.95	3.27
		XRL/s (Downstream)	4.74	6.25	6.34	4.77
	CR 0.70	XRL/s (Upstream)	1.67	1.06	1.07	1.67
		XRL/s (Downstream)	2.98	4.37	4.77	3.00
	CR 0.55	XRL/s (Upstream)	1.173	0.853	0.876	1.171
		XRL/s (Downstream)	2.17	3.04	3.56	2.24
Reynolds Number	**Re 5000**	XRL/s (Upstream)	1.62	0.85	0.85	1.62
		XRL/s (Downstream)	2.58	2.57	2.59	2.58
	Re 7000	XRL/s (Upstream)	1.67	1.05	1.07	1.64
		XRL/s (Downstream)	2.93	4.37	4.78	2.94
	Re 10000	XRL/s (Upstream)	1.833	1.660	1.673	1.833
		XRL/s (Downstream)	2.97	4.67	4.80	3.28
Prandtl Number	**Air**	XRL/s (Upstream)	1.67	1.05	1.07	1.67
		XRL/s (Downstream)	2.58	2.57	2.59	2.71
	Water	XRL/s (Upstream)	1.83	1.22	1.67	1.83
		XRL/s (Downstream)	2.98	4.37	5.50	2.96
	Oil	XRL/s (Upstream)	2.000	1.660	2.380	2.150
		XRL/s (Downstream)	3.18	5.90	6.53	3.28

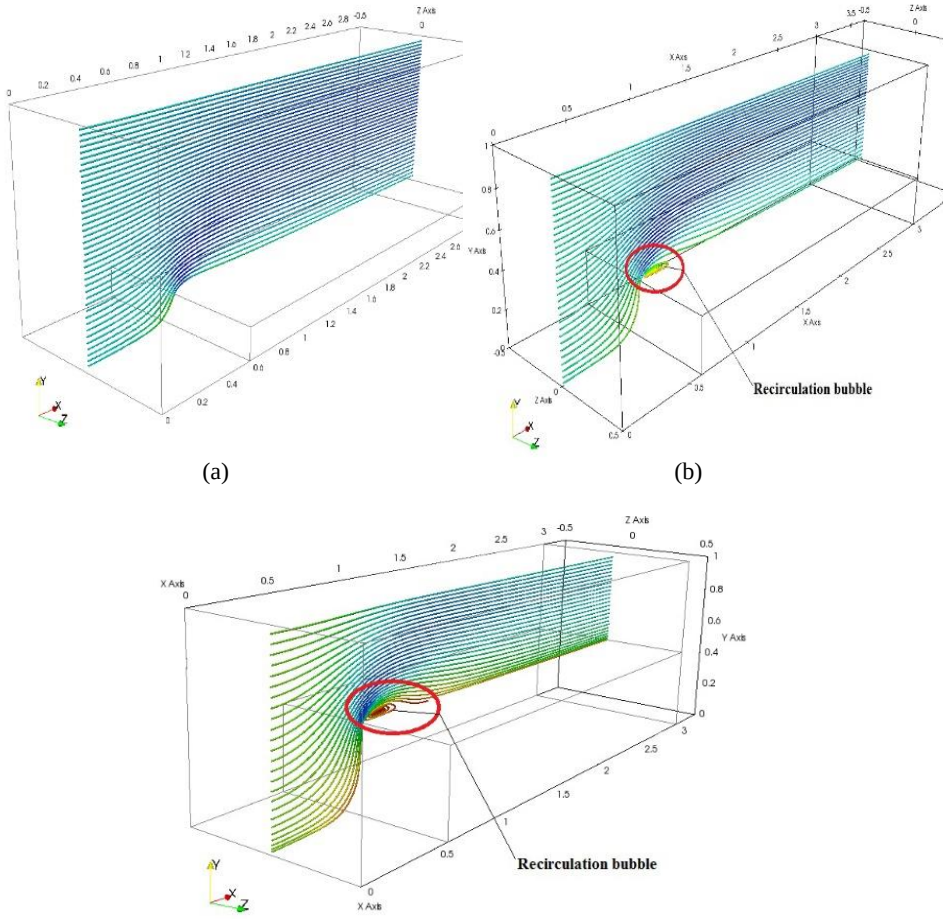

(a) (b)

(c)

Figure 5 (a)-(c) Velocity streamline in the downstream region for the k-ε model. (a) CR = 0.85, (b) CR = 0.70, (c) CR = 0.55; (a)-(c) Re = 7000, Pr = 0.71.

The distribution of C_f in the bottom surface (x-z plane) in the downstream region for the different turbulence models is shown in Figure 6. The portions encircled in the C_f contour plot show the recirculation region; all values have a positive sign. In this region, the fluid flow and the wall shear stress act in the same direction, hence the C_f values are positive. Nevertheless, when the direction of the wall shear stress changes, the C_f values change to a negative sign. The contours of the k-ε and v^2-f models show the same trend. Figure 7 shows a graphical representation of C_f along the centerline of the heated upstream and downstream walls. From Figures 7 (a) and (b) it is clear that in the upstream and downstream regions, the values of the skin friction coefficient increased with step height and due to the presence of the recirculation region, the C_f sign changed from positive

to negative. Simulations with different turbulence models showed that, since the wall shear stress values were almost the same, the variation of C_f was similar for the k-ε and v^2-f models. However, for the k-ω and k-ω *SST* models, due the over-predicting behavior, the C_f values were higher compared to those for the k-ε and v^2-f models.

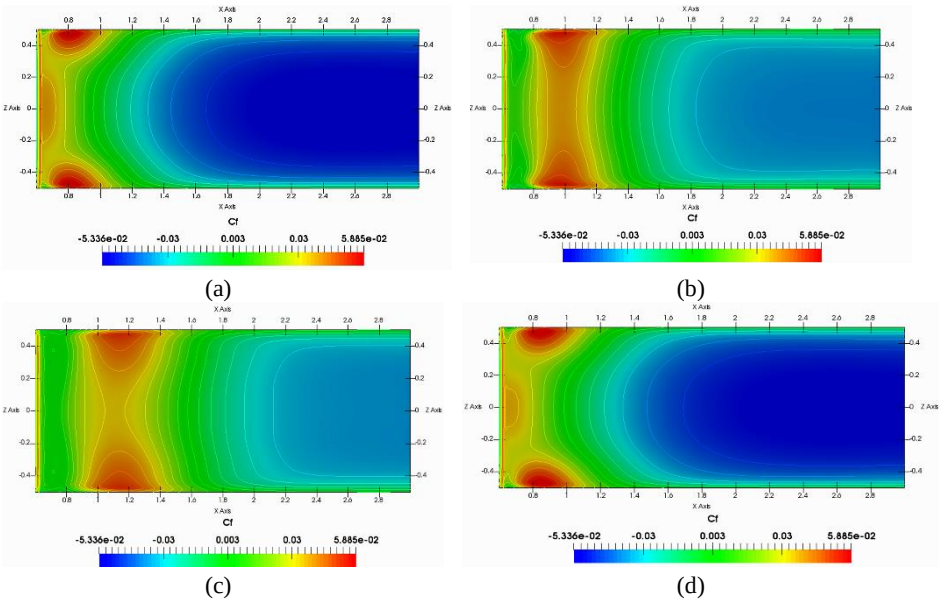

Figure 6 (a) - (d) C_f contours in the downstream region. (a) k-ε, (b) k-ω, (c) k-w *SST*, (d) v^2-f; (a) - (d) CR = 0.55, Re = 7000, Pr = 0.71.

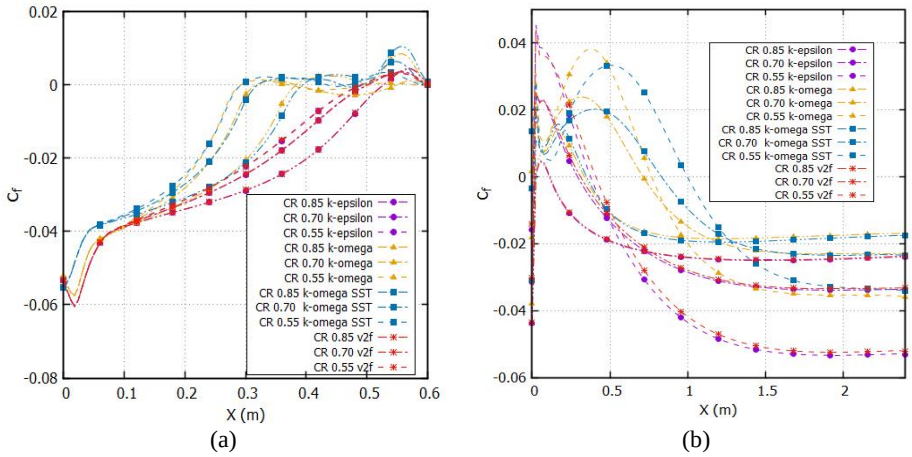

Figure 7 C_f distribution for the k-ε, k-ω, k-ω *SST* and v^2-f turbulence models for CR = 0.85, 0.70 and 0.55: (a) on the upstream wall, (b) on the downstream wall.

The variation of static pressure coefficient C_p along the centerline on the upstream and downstream walls is shown in Figure 8. The pressure coefficient was positive in the upstream region for all contraction ratios and turbulence models. The C_p value increased with step height, which is due to the increase in recirculation length. For contraction ratio 0.85, variation was very small compared to contraction ratio 0.55.

The C_p values were negative in the downstream region for all cases, as shown in Figure 8(b). The Nusselt number distribution along the centerline in the upstream and downstream walls are shown in the Figure 9. In the upstream region, before the recirculation zone, Nu values were higher for all contraction ratios.

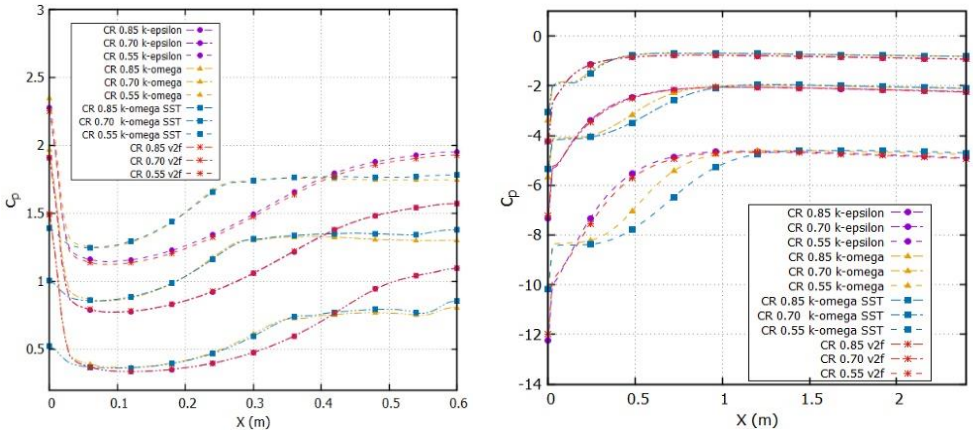

Figure 8 Cp distribution for the *k-ε*, *k-ω*, *k-ω SST* and v^2-*f* turbulence models for CR = 0.85, 0.70 and 0.55: (a) on the upstream wall, (b) on the downstream wall.

However, upon reaching the recirculation bubble in the upstream region, the Nu values became lower due the smaller heat flux, as is clearly shown in Figure 9(a). All four turbulence models showed the same trend in the upstream region. The peak in Figure 9(b) indicates the maximum value for Nu in the downstream region, where the second reattachment takes place. In this region, the heat flux due to wall heating was maximum.

After the peak region, the Nu variation shows a linear trend, where the flow is without any recirculation. For all turbulence models, as the contraction ratio decreased, the Nu value increased in the reattachment zone of the downstream wall, mainly due to the blockage effect of the step wall and the subsequent heat transfer in the step wall region.

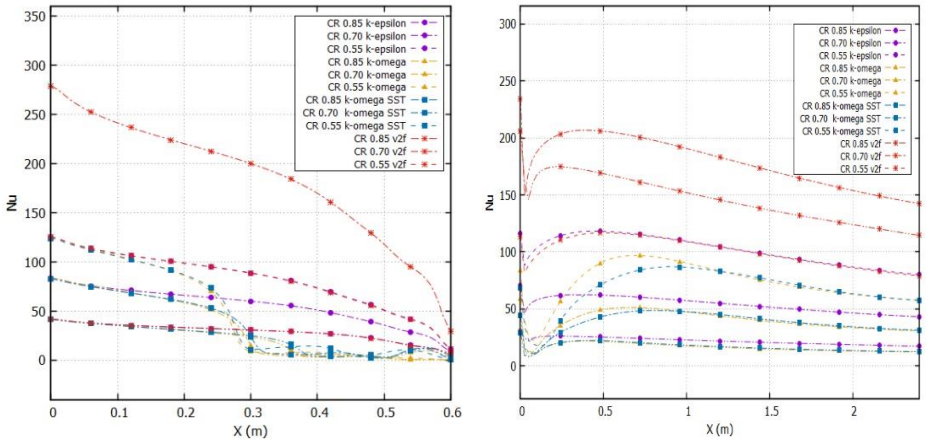

(a) (b)

Figure 9 Nu distributions for different CR values and turbulence models: (a) on the upstream wall, (b) on the downstream wall.

5.2 Reynolds Number

The effects of the Reynolds number on the flow and heat transfer characteristics over an FFS are discussed in this section. For this analysis, a FFS with CR = 0.70 and fluid with Pr = 0.71 was considered. It is observed that for both the *k-ε* and v^2*-f* turbulence models by increasing the Re value from 5000 to 10,000, the recirculation length in the upstream region increased by 11.81%. However, for the *k-ω* and *k-ω SST* models the increment was in the order of 48.6% and 49.2%, respectively. In the downstream region, when using the *k-ε* and v^2*-f* turbulence models with increasing Re value, the recirculation length increased by 13.13% and 21.44%, respectively. However, under the same conditions, the *k-ω* and *k-ω SST* models showed an increment of the recirculation length in the order 44.85% and 45.97%, respectively. Therefore it can be stated that for all the turbulence models, with an increase in the Reynolds number the values of the recirculation length on the upstream and downstream walls increased, thereby increasing the heat transfer rate.

Figure 10 shows the variation of C_f along the centerline on the upstream and downstream walls. From Figure 10(a) it is clear that the C_f value increased with the Reynolds number for all four turbulence models. However, the *k-ε* and v^2*-f* models showed the same results for all different Re values. From the numerical analysis it can be seen that with an increase of the Reynolds number the value of the recirculation length on the upstream and downstream walls increased, thereby increasing the heat transfer rate. From Figure 10 (a) and (b) it is clear that in the upstream and downstream regions, the value of the skin friction coefficient increased with the Re value and due to the presence of the recirculation region,

the C_f sign changed from positive to negative. The peak value of C_f in Figure 10(b) indicates the reattachment point in the downstream region, where the shear stress values are high. After this point, the C_f value decreased and remained constant for all four turbulence models, indicating that the flow was fully developed. The C_f variations were similar for the *k-ε* and v^2-*f* turbulence models.

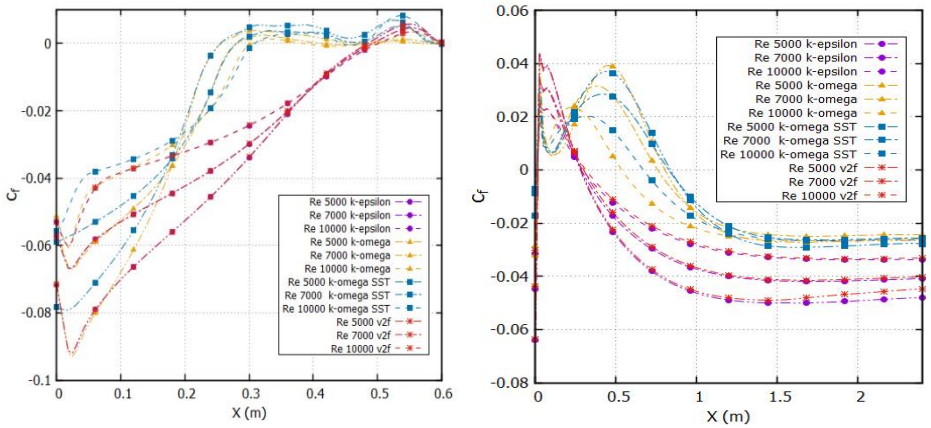

(a) (b)

Figure 10 C_f distribution for the *k-ε*, *k-ω*, *k-ω SST* and v^2-*f* turbulence models for different Re values: (a) on the upstream wall, (b) on the downstream wall.

Figure 11 shows the distribution of Nu for the different values of Re and the turbulence models on the downstream wall. The figure shows that the Nusselt number decreases in the recirculation region, where the wall heat flux is lower.

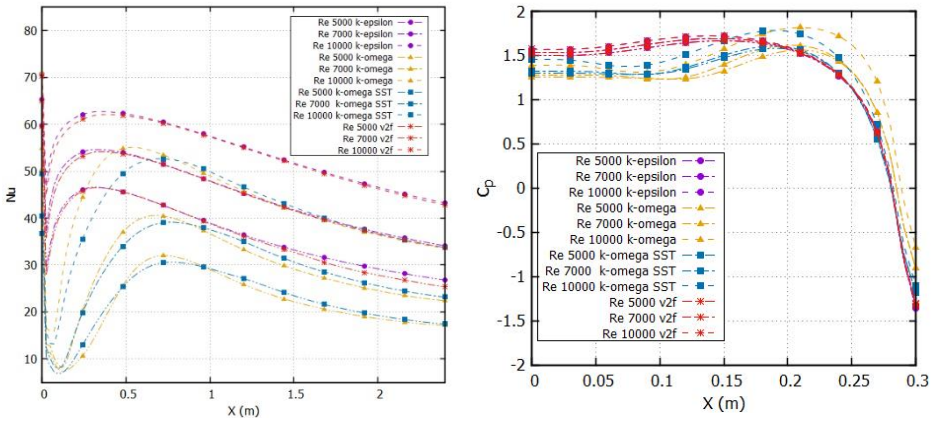

(a) (b)

Figure 11 (a) Nu distribution on downstream wall for the *k-ε*, *k-ω*, *k-ω SST* and v^2-*f* turbulence models and different Re values. (b) C_p distribution on the step wall for the *k-ε*, *k-ω*, *k-ω SST* and v^2-*f* turbulence models and different Re values.

Table 1 shows the variations in recirculation length for different turbulence models and Re values. Upon reaching the reattachment zone in the downstream region, the Nu values were higher. Since *k-ω* and *k-ω SST* over-predict the values of the recirculation length, the Nu values for these models were higher compared to the *k-ε* and v^2*-f* models.

5.3 Prandtl Number

In order to analyze the effect of the Prandtl number on the flow and heat transfer characteristics of FFS, three working fluids, viz., air, water and oil were taken. An Re value of 7000 and an FFS with contraction ratio 0.70 were considered for the simulations. The current simulations indicate that due to variations in the value of Pr major changes occur in the step region.

Figure 12 (a), (b) and (c) show the variations of the skin friction coefficient, the pressure coefficient and the Nusselt number along the centerline of the heated step wall. Due to the effect of the recirculation zones on the upstream and downstream walls, the C_f and C_p values in the step region change their sign from positive to negative, as can be seen from Figures 12 (a) and (b).

At higher a Prandtl number, the values of the recirculation length were higher, thereby giving higher C_f and C_p values. It can be observed that as the Prandtl number increased, the convective heat transfer coefficient increased for all four turbulence models.

The results reveal that *k-ω* and *k-ω SST* over-predict the recirculation length in the downstream region. Hence, the Nu values for these models were higher compared to those for the *k-ε* and *v2-f* models.

The quantitative results of the present work show that for the k-ε and v2-f models, by changing the working fluid from air to oil the recirculation length in the upstream region increased by 16.33% and 22.48%, respectively. However, for the *k-ω* and *k-ω SST* models the increments were in the order 36.75% and 55.04%, respectively.

In the downstream region, the simulations with the *k-ε* and v^2*-f* models showed an increment of 18.95% and 17.28% in the recirculation length when the working fluid was changed from air to oil. However, for the *k-ω* and *k-ω SST* models the increment of the recirculation length in the downstream region was in the order of 56.38% and 60.31%, respectively.

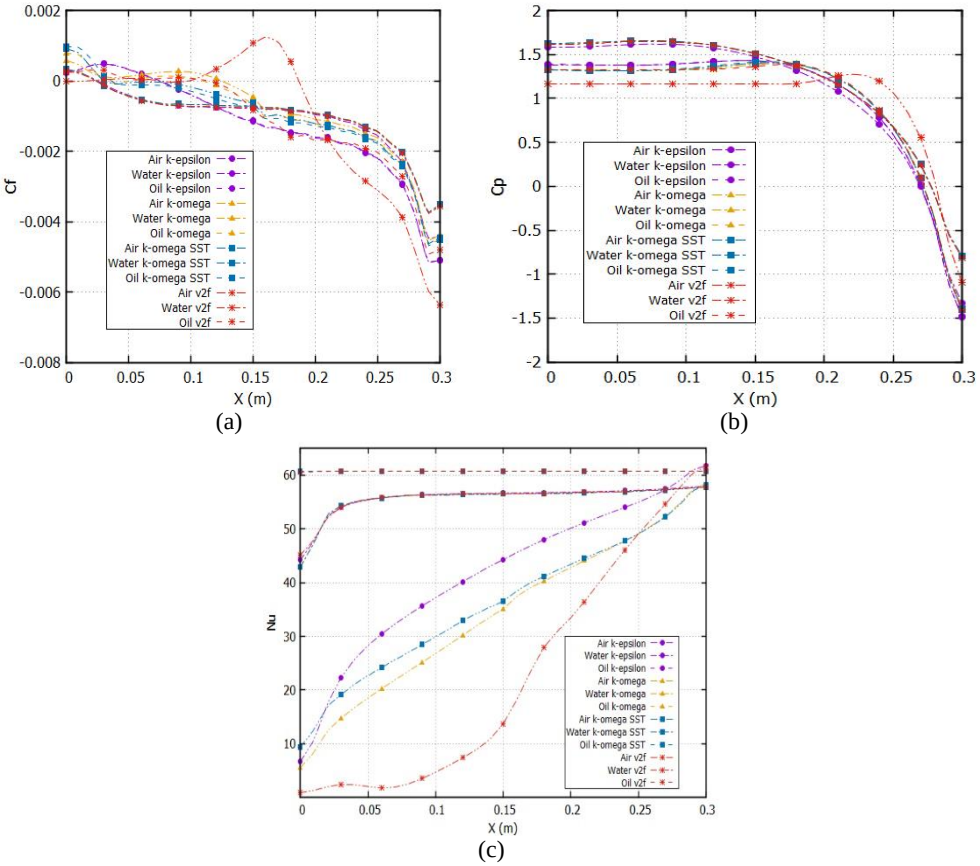

Figure 12 (a) C_f distribution over the step. (b) C_p distribution over the step. (c) Nu distribution over the step. 15 (a)-(c) for the *k-ε*, *k-ω*, *k-ω SST* and v^2-*f* turbulence models with different Pr values.

6 Conclusions

In this work, a newly developed transient incompressible solver pisoTempFoam in the OpenFOAM 4.1 framework was used for analyzing the convective heat transfer characteristics over a heated forward facing step. The newly developed solver was validated. From the present numerical analysis, it can be seen that when using the *k-ε* and v^2-*f* turbulence models, for an increment in step height, the recirculation length in the upstream region was increased by 6.97%. However, for the *k-ω* and *k-ω SST* models, the increment in the recirculation length for an increase in step height were in the order of 23.96% and 25.63%, respectively. The quantitative analysis of the recirculation length proved that in the downstream region, when using the *k-ε* and v^2-*f* turbulence models, with an increment in step height the recirculation length increased by 27.23% and 29.21, respectively. It

was observed that, for both the k-ε and v^2-f turbulence models, increasing the Re value, the recirculation length in the upstream region increased by 11.81%. Nevertheless, for the k-ω and k-ω *SST* models the increment of the recirculation length with an increase in Re was in the order of 48.59% and 49.203%, respectively. The flow visualization results indicated that in the downstream region, by changing the Re value from 5,000 to 10,000, the recirculation length increased by 13.13% and 21.44%, respectively, for the k-ε and v^2-f turbulence models.

The results of the present work showed that, for both the k-ε and v^2-f turbulence models, by changing the working fluid from air to oil, the recirculation length in the upstream region increased by 16.33% and 22.48%, respectively. However, for the k-ω and k-ω *SST* models the increment of the recirculation length by changing the working fluid was in the order of 36.75% and 55.04%, respectively. From the present numerical analysis it is concluded that each turbulence model shows its own behavior related to the fluid flow and heat transfer characteristics. However, compared to the other two turbulence models (k-ω and k-ω *SST*), when using k-ε and v^2-f, the validation and numerical results got better adherence. Therefore, under the given conditions, the k-ε and v^2-f models proved to be better suited turbulence models for analyzing the flow and heat transfer characteristics over a 3D FFS.

References

[1] Vogel, J.G. & Eaton, J.K., *Combined Heat Transfer and Fluid Dynamic Measurements Downstream of a Backward-Facing Step*, Transactions of the ASME, Journal of Heat Transfer, **107**, pp. 922-928, 1985.

[2] Jayakumar, J.S., Kumar, I. & Eswaran, V., *Hybrid Mesh Finite Volume* CFD *Code for Studying Heat Transfer in a Forward-Facing Step*, Physica Scripta. **142,** 014060, pp. 1-11, 2010.

[3] Sajesh, P. & Jayakumar, J.S., *Effect of Streamline Curvature on Heat Transfer in Turbulent Flow over Backward Facing Step*, 3rd International Conference on Advances in Materials and Manufacturing Applications (IConAMMA 2018), 16th - 18th August 2018.

[4] Vijay, A., Nitish,C.N., Subash, A., Raj,S., Kumar S.,A. &Jayakumar, J.S., *Numerical Simulation on Flow over a Double Forward Facing Step*, AIP Conference Proceedings, **2134**, 040004, pp. 1-6, 2019. DOI: 10.1063/1.5120212.

[5] Hussein, T., Ahmadi, G., Tuqa, A., Ahmed, J.S., Kazi, S.N., Badarudin, A. & Safaei, M.R., *Thermal Performance of Nanofluid in Ducts with Double Forward-Facing Steps*, Journal of the Taiwan Institute of Chemical Engineers, **47**, pp. 28-42, 2015. DOI: 10.1016/ j.jtice.2014.10.009

[6] Safaei, M.R., Hussein Togun., Vafai, K., Kazi, S.N. & Badarudin, A., *Investigation of Heat Transfer Enhancement in a Forward-Facing Contracting Channel Using FMWCNT Nanofluids,* Numerical Heat Transfer, Part A: Applications: An International Journal of Computation and Methodology, **66**, pp. 1321-1340, 2014. DOI: 10.1080/ 10407782.2014.916101.

[7] Alrashed, A.A.A.A., Akbari, O.A., Heydari, A., Toghraie, D., Zarringhalam, M., Shabani, G.A.S., Seifi, A.R. & Goodarzi, M., *The Numerical Modeling of Water/FMWCNT Nanofluid Flow and Heat Transfer in a Backward-facing Contracting Channel*, Physica B: Physics of Condensed Matter, **537**, pp. 176-183, 2018.

[8] Kherbeet, A. S., Mohammed, H.A., Hamdi, E. A., Salmand, B.H., Omer, A.A., Mohammad, R.S. & Khazaal, M.T., *Mixed Convection Nanofluid Flow over Microscale Forward-Facing Step – Effect of Inclination and Step Heights*, International Communications in Heat and Mass Transfer, **78**, pp. 145-154, 2016. DOI: 10.1016/j.icheatmasstransfer.2016.08.016.

[9] Eka, O.N. & Syunsuke, I., *Comparison Study of Flow in a Compound Channel: Experimental and Numerical Method Using Large Eddy Simulation SDS-2DH Model*, ITB Journal of Engineering Sciences, **39**, pp. 67-97, 2007. DOI: 10.5614/itbj.eng.sci.2007.39.2.1.

[10] Kusuma, M.S.B., Rani, A., Anom, R. & Cahyono, M., *Development Study of Turbulent k- ε Model for Recirculation Flow III: Two Dimension Recirculation Flow in a Reservoir*, ITB Journal of Engineering Science, **41**, pp. 1-16, 2009. DOI: 10.5614/ itbj.eng.sci.2009.41.1.1.

[11] Li, Z.Y., Guo, S., Bai, H.L. & Gao, N., *Combined Flow and Heat Transfer Measurements of Backward Facing Step Flows Under Periodic Perturbation*, International Journal of Heat and Mass Transfer, **130**, pp. 240-251, 2019.

[12] Ali, K.H., Abd Rahim, A.T., Antonio, A.I., Mohammed, T.H.S. & Mohd Faisal, A.H., *Effect of Corrugated Wall Combined with Backward-Facing Step Channel on Fluid Flow and Heat Transfer*, Energy, **190**, pp. 1-10, 2020. DOI: 10.1016/j.energy.2019.116294.

[13] Greenshields, C.J., *OpenFOAM User Guide*, Version 4.1, 2017.

[14] Greenshields, C.J., *OpenFOAM Programmer's Guide*, Version 4.1, 2017.